

Gravitational wave extraction based on Cauchy-characteristic extraction and characteristic evolution

Maria Babiuc,¹ Béla Szilágyi,^{1,2} Ian Hawke,^{2,3} and Yosef Zlochower⁴

¹*Department of Physics and Astronomy, University of Pittsburgh, Pittsburgh, PA 15260, US*

²*Max-Planck-Institut für Gravitationsphysik, Albert-Einstein-Institut, Am Mühlenberg 1, D-14476 Golm, Germany*

³*School of Mathematics, University of Southampton, Southampton SO17 1BJ, UK*

⁴*Department of Physics and Astronomy, and Center for Gravitational Wave Astronomy,
The University of Texas at Brownsville, Brownsville, TX 78520, US*

(Dated: Date: 2004/12/13 12:14:49)

We implement a code to find the gravitational news at future null infinity by using data from a Cauchy code as boundary data for a characteristic code. This technique of *Cauchy-characteristic Extraction* (CCE) allows for the unambiguous extraction of gravitational waves from numerical simulations.

PACS numbers: 04.25.Dm, 95.30.Sf, 97.60.Lf

I. INTRODUCTION

The need of gravitational waveform templates for gravitational wave detectors implies a need for accurate 3D numerical simulations of isolated sources such as binary black hole mergers. These simulations are often done with Cauchy codes (based on a “3+1” slicing of spacetime). The nature of the majority of these slicing conditions, e.g. maximal slicing, implies that one would have to evolve spacetime to $t = 1$ in order to obtain information, such as the gravitational news, at future null infinity \mathcal{I}^+ [38]. As this is not computationally possible various approximations are used to extract gravitational waves.

An alternative approach is to match the Cauchy evolution code to another code based on outgoing characteristics. By construction, these characteristic slices connect the region evolved by the “3+1” code with \mathcal{I}^+ at each time-step and naturally describe the radiation-region of the physical system. It is then not necessary to evolve the Cauchy slice for infinitely long times in order to obtain the gravitational wave signal via an accurate numerical algorithm. In addition to calculating the gravitational waveform at \mathcal{I}^+ , in Cauchy-Characteristic Matching (CCM) one can also use data from the characteristic evolution to provide boundary data for the Cauchy evolution. CCM has proved successful in numerical evolution of the spherically symmetric Klein-Gordon-Einstein field equations [1], for 3-D non-linear wave equations [2] and for the linearized harmonic Einstein system [3].

In this work the radiation-region is numerically described by the Pitt Null Code [1, 4, 5, 6, 7, 8, 9, 10]. The link between the Cauchy and the characteristic (or Bondi) codes is done by a non-linear 3D Cauchy-characteristic extraction (CCE) algorithm the first version of which had been developed by the PITT team [6, 10, 11, 12]. At the outer edge of the Bondi code a News Extraction module (NE) is used to calculate the gravitational news [5, 8, 13, 14]. Here the combined CCE-NE codes have been imported into the Cactus computational infrastructure [15, 16, 17, 18]. Within this infrastructure we have been able to use two separate Cauchy codes implementing two completely different formulations of the 3 + 1 split Einstein equations. This allows us to test the robustness of the CCE approach. In addition, we have also compared the results of the CCE algorithm and of the Zerilli approximation [19, 20, 21]. The comparison gave results consistent with reference [22]: the CCE algorithm is $\mathcal{O}(\Delta x^2)$ accurate (where Δx is the computational grid-step), while the accuracy of the perturbative (Zerilli) approach is $\mathcal{O}(r^{-2})$ where r is the radius of the wave extraction sphere. In addition, it is shown in [22] that the computational intensity of CCE relative to that of the perturbative approach goes to zero as the desired error goes to zero.

This paper is arranged as follows. In Sec. II we outline some general background and notation. In Sec. III we detail the transformation from the Cauchy slice to the characteristic slice. In Sec. IV we give a brief summary of the characteristic evolution code. In Sec. V we describe how the news is computed at \mathcal{I}^+ . Finally, in Sec. VI we give a number of tests in full 3D numerical relativity to validate the accuracy, convergence and robustness of the CCE algorithm.

II. NOTATION, GEOMETRY AND METRICS

The implementation of CCE described here follows previous descriptions of Cauchy-characteristic extraction and matching in the literature. Much of the work has been presented earlier, e.g. [6, 10, 11, 12]. Here we briefly outline the notation, geometry and metrics used.

The geometry is described by two separate foliations, neither of which cover the entire spacetime. The Cauchy foliation is described using a standard 3 + 1 ADM type metric [23],

$$ds^2 = -(\alpha^2 - \beta_i \beta^i) dt^2 + 2 \beta_i dt dx^i + \gamma_{ij} dx^i dx^j : \quad (2.1)$$

Many different formulations can be used, given initial and boundary data, to evolve the 3-metric g_{ij} . In what follows we shall either consider the BSSN formulation ([24, 25]) as implemented in [26] or the generalized harmonic formulation ([27]) as implemented in the Abigel code [27]. In both cases all interaction between the Cauchy and characteristic foliations will be performed in terms of the ADM metric, Eq. (2.1).

The Cauchy slice does not extend to asymptotic infinity. Instead an artificial boundary is placed at $x^i = L^i$. Within this artificial boundary a *world-tube* is constructed such that its intersection with any $t = \text{const.}$ Cauchy slice is defined as a Cartesian sphere $x^2 + y^2 + z^2 = R^2$, with angular coordinates labeled by $y^A; A = [2; 3]$. The world-tube is then used as the inner boundary of a characteristic foliation which uses the standard Bondi-Sachs metric [28, 29]

$$ds^2 = -e^2 \frac{V}{r} (r^2 h_{AB} U^A U^B du^2 - 2e^2 du dr - 2r^2 h_{AB} U^B dy^A + r^2 h_{AB} dy^A dy^B) : \quad (2.2)$$

Here u labels the outgoing null hypersurfaces, $y^A = y^{\bar{A}}$ the null rays emanating from the world-tube, and r is a radial surface area distance. h_{AB} satisfies

$$h^A{}_B h_B{}_C = \delta^A_C \quad (2.3)$$

and

$$\det(h_{AB}) = \det(q_{AB}) \quad (2.4)$$

where q_{AB} is the unit sphere metric. This coordinate system consistently covers the world-tube and the exterior spacetime as long as it is free of caustics.

The free variables in the Bondi-Sachs metric are then $V; y^A$ and h_{AB} . The physical interpretation of these variables is that h_{AB} contains the 2 radiative degrees of freedom, e^2 measures the expansion of the nullcone between an asymptotic frame and the world-tube, and V is the analog of the Newtonian potential. For further insight, one can write the intrinsic metric of the $r = \text{const.}$ surfaces as

$$g_{ij} dy^i dy^j = -e^2 \frac{V}{r} du^2 + r^2 h_{AB} (dy^A - U^A du) (dy^B - U^B du) : \quad (2.5)$$

This 2+1 decomposition of the timelike world-tube geometry identifies $r^2 h_{AB}$ as the metric of the 2-surfaces (Bondi spheres) of constant u , with U^A being the shift vector. The square of the lapse function is $e^2 V = r$.

III. THE CCE ALGORITHM

The crucial task of the CCE algorithm is to take Cauchy data given in the ADM form (2.1) in a neighborhood of the world-tube and transform it into boundary data for the Bondi-Sachs metric (2.2). Then the Bondi code can use the hypersurface equations to evolve the appropriate quantities out to \mathcal{I}^+ so that the gravitational news may be extracted there. Much of the present version of the CCE algorithm has been presented in earlier work [6, 10, 11, 12], so in this section we will give a brief description, highlighting a few new features.

In section II the world-tube was defined as a Cartesian sphere $x^2 + y^2 + z^2 = R^2$, with angular coordinates labeled by $y^A; A = [2; 3]$. In addition to the angular coordinates we set $u = t$ on the world-tube and choose the fourth coordinate, to be an affine parameter along the radial direction, with $u_j = 0$. The characteristic cones are constructed such that the direction is future oriented, outgoing null and normal to Σ . (In order to avoid a singular Jacobian for the Cauchy-characteristic coordinate transformation, we require that the world-tube be timelike.) The affine parameter is used because the world-tube as constructed is not a surface of constant Bondi r .

The choice of the angular coordinates is determined following [30] by the use of two stereographic patches. These are centered around the North and South poles with the stereographic coordinates related to the usual spherical $(\theta; \phi)$ by

$$r_{\text{North}} = \frac{r}{1 + \cos \theta} e^{i\phi}; \quad r_{\text{South}} = \frac{r}{1 - \cos \theta} e^{-i\phi}; \quad (3.1)$$

and $\bar{y}^2 + \bar{y}^3 = q + \bar{p}$; where $\bar{p} = \frac{P}{1 + P^2}$. We also introduce the complex vector on the sphere $q^A = (P=2) \left(\frac{A}{2} + \bar{p} \frac{A}{3} \right)$ and its co-vector $q_A = (2=P) \left(\frac{A}{2} + \bar{p} \frac{A}{3} \right)$, with $P = 1 + \bar{p}^2 = 1 + q^2 + p^2$. The orthogonality condition $q_A q^A = 2$ is satisfied by construction. The unit sphere metric corresponding to these coordinates is

$$q_{AB} = \frac{1}{2} (q_A q_B + \bar{q}_A \bar{q}_B) = \frac{4}{P^2} \begin{pmatrix} 1 & 0 \\ 0 & 1 \end{pmatrix} \quad (3.2)$$

The angular subspace in the Bondi code is treated by use of the *eth* formalism and spin-weighted quantities. (See [8, 30] for details.)

The CCE algorithm starts by interpolating the Cauchy metric g_{ij} , lapse and shift i and their spatial derivatives onto the world-tube. Time derivatives are computed via backwards finite-differencing done along t , e.g., at $t = t_N$ we write

$$(\partial_t F)_{[N]} = \frac{1}{2\Delta t} (3F_{[N]} - 4F_{[N-1]} + F_{[N-2]}) + O(\Delta t)^2 \quad (3.3)$$

Knowledge of the Cauchy metric and its 4-derivative is enough to compute the affine metric $\tilde{\gamma}_{AB}$ as a Taylor series expansion around the world-tube:

$$\tilde{\gamma}_{AB} = \tilde{\gamma}_{AB}^j + \tilde{\gamma}_{AB}^{;j} + O(\Delta t^2) \quad (3.4)$$

Next a second null coordinate system (the Bondi-Sachs system) is introduced:

$$y = (y^1; y^A; y^4); \text{ where } y^A = \tilde{y}^A; \quad y^1 = \tilde{y}^1 = u: \quad (3.5)$$

The fourth coordinate $y^4 = r$ is a surface area coordinate, defined by

$$r = \frac{\det(\tilde{\gamma}_{AB})}{\det(q_{AB})}^{\frac{1}{4}} = \frac{P}{2} \det(\tilde{\gamma}_{AB})^{\frac{1}{4}} \quad (3.6)$$

The Bondi-Sachs metric on the extraction world-tube can be computed as

$$g_{ij} = \frac{\partial y}{\partial \tilde{y}^i} \frac{\partial y}{\partial \tilde{y}^j} \tilde{\gamma}_{AB} \quad (3.7)$$

Note that the metric on the sphere is unchanged by this coordinate transformation, i.e., ${}^{AB} = \tilde{\gamma}^{AB}$. Therefore one only needs to work with the Jacobian components that correspond to derivatives of r .

In terms of $q^A; q^A$ the two dimensional metric AB can be encoded into the metric functions

$$J = \frac{1}{2} q^A q^B h_{AB}; \quad K = \frac{1}{2} q^A q^B h_{AB} : \quad (3.8)$$

The determinant condition Eq. (2.4) translates into

$$K^2 = 1 + JJ : \quad (3.9)$$

With h_{AB} symmetric and of fixed determinant, there are only two degrees of freedom in the angular metric that are encoded into the complex function J .

From Eq. (2.2) we have

$$= \frac{1}{2} \log(r_r) = \frac{1}{2} \log(r;) \quad (3.10)$$

This quantity is a measure of the expansion of the light rays as they propagate outwards. The CCE and the Bondi codes have been implemented with the assumption that $r_r > 0$ (or that r is real).

The radial-angular components rA can be represented by

$$U = U^A q_A = \frac{r_A}{r_u} \quad (3.11)$$

while the radial-radial component rr is contained in

$$W = \frac{V}{r^2} r : \quad (3.12)$$

In addition to these quantities, in [9] the auxiliary variables

$$gJ = \frac{1}{2} h_{AB} ;_C q^A q^B q^C \quad (3.13)$$

$$k = gK = \frac{1}{2} h_{AB} ;_C q^A q^B q^C + 2K \quad (3.14)$$

$$B = g = ;_A q^A \quad (3.15)$$

have been introduced to eliminate the need to explicitly use second angular derivatives in the Bondi evolution code. The required boundary data is $\mathcal{J}; \mathcal{U}; \partial_r \mathcal{U}; \mathcal{W}; \mathcal{K};$ and \mathcal{B} . (See Sec. IV.) Notice that once the Bondi-Sachs metric is known on the world-tube one can only obtain $\mathcal{J}; \mathcal{U}; \mathcal{W}$. In order to provide the rest of the necessary boundary data we need the radial derivative of the Bondi-Sachs metric

$$(\partial_r \mathcal{U})_j = \frac{\partial^2 \mathcal{Y}}{\partial \mathcal{Y}^{\sim} \partial \mathcal{Y}^{\sim}} \frac{\partial \mathcal{Y}}{\partial \mathcal{Y}^{\sim}} \sim \sim + \frac{\partial \mathcal{Y}}{\partial \mathcal{Y}^{\sim}} \frac{\partial^2 \mathcal{Y}}{\partial \mathcal{Y}^{\sim} \partial \mathcal{Y}^{\sim}} \sim \sim + \frac{\partial \mathcal{Y}}{\partial \mathcal{Y}^{\sim}} \frac{\partial \mathcal{Y}}{\partial \mathcal{Y}^{\sim}} \sim; \sim_j \quad (3.16)$$

With $\sim; \sim$ already known, the only non-trivial parts in Eq.(3.16) are the Jacobian terms

$$r; \sim = \frac{\partial^2 \mathcal{Y}^1}{\partial \mathcal{Y}^{\sim}} : \quad (3.17)$$

These depend on the second derivatives of the Cauchy metric. In order to avoid possible numerical problems caused by interpolating second derivatives onto the world-tube, we calculate $r; \sim$ by taking centered derivatives of $r;$ on the world-tube and we calculate $r; \sim$ by backwards differencing in time along the world-tube. The remaining term $r;$ is calculated using the identity

$$; = \frac{r;}{2 r;} \quad (3.18)$$

and the characteristic equation

$$r = \frac{r}{8} \mathcal{J}_{;r} \mathcal{J}_{;r} - (\mathcal{K}_{;r})^2 : \quad (3.19)$$

(The right hand side of Eq. (3.19) can be computed in terms of $\mathcal{J}_{;r} = \mathcal{J}; r;$, which, in turn, can be computed in terms of already known quantities.)

Knowledge of the radial derivative of the Bondi metric is important not only for obtaining $(\partial_r \mathcal{U})_j$ but also because the grid-structure of the Bondi code is based on the radial coordinate r , and the extraction world-tube will not, in general, coincide with any of these radial grid-points. We need to use, therefore, Taylor series expansions to fill the Bondi gridpoints surrounding with the necessary boundary data. We write, e.g.,

$$= j + ; + O(\Delta^2) \quad (3.20)$$

Another problem is the need to provide the auxiliary angular variables, $\mathcal{B}; \mathcal{K}$ and \mathcal{B} on the world-tube. These have been defined as the g -derivatives of Bondi fields in the \mathcal{Y} frame, while taking angular derivatives on the world-tube amounts to computing g derivatives in the \mathcal{Y}^{\sim} frame. The correction term between the two frames is

$$gF = \tilde{g}F + \frac{F_i}{r_i} \tilde{g}r \quad (3.21)$$

The quantities $\mathcal{J}; \tilde{g}\mathcal{J}$ and $\mathcal{J};$ are known from the interpolated Cauchy data, while $\mathcal{J};$ is not computed in CCE. Thus one can compute $g\mathcal{J}$ but not $g\mathcal{J};$. As a consequence we cannot use a simple Taylor series expansion to place \mathcal{J} on the Bondi grid to $O(\Delta^2)$ accuracy. The solution to this problem is to first place \mathcal{J} on Bondi grid-points surrounding the world-tube, then compute $g\mathcal{J}$ on those points (i.e., compute angular derivatives in the Bondi-Sachs frame), and then calculate $\partial_r g\mathcal{J}$ on the world-tube by use of the neighboring Bondi grid values of $g\mathcal{J}$. With $\mathcal{J} = g\mathcal{J}$ and its radial derivative known on the world-tube, we can then use the standard $O(\Delta^2)$ expansion to provide \mathcal{J} at Bondi gridpoints surrounding the world-tube. This way we make maximal use of the Cauchy data as interpolated onto the world-tube and minimal use of the finite difference g algorithm that has its own discontinuous $O(\Delta^2)$ error at the edges of the stereographic patches. A similar approach is used for $\mathcal{K} = g\mathcal{K}$ and $\mathcal{B} = g\mathcal{B}$.

IV. THE BONDI CODE

The inner workings of the Bondi code had been described in detail elsewhere (see [1, 4, 5, 6, 7, 8, 9, 10]) so here we give only a brief overview of the algorithm. As already stated in Sec. III, the variables of the code are $\mathcal{J}; \mathcal{U}; \mathcal{W}$ as well as $\mathcal{K}; \mathcal{B}$. Out of these the equation for \mathcal{J} is the only one to contain a time derivative. For this reason \mathcal{J} is updated via an evolution stencil that involves two time-levels. The rest of the variables are integrated radially from the world-tube out to \mathcal{I}^+ . The integration constants are set by CCE. All of these radial integration equations are first differential order in r except for the \mathcal{U} equation which contains $\mathcal{U}_{;r}$. For this reason integrating \mathcal{U} requires two constants, which explains the need to provide, at the world-tube, \mathcal{U} as well as $\mathcal{U}_{;r}$.

V. THE NEWS ALGORITHM

The calculation of the Bondi News function on \mathcal{I}^+ is based on the algorithm developed in [8] with the modifications introduced in [13, 14] (an alternative calculation for the News was recently introduced in [31]). Here we present an overview of the algorithm.

The Bondi-Sachs metric (2.2) in a neighborhood of \mathcal{I}^+ in $(u; x^A; l = 1-r)$ coordinates (after multiplying by a conformal factor \mathcal{L}^2) has the form

$$\mathcal{L}^2 ds^2 = \mathcal{O}(\mathcal{L}^2) du^2 + 2e^2 du dl - 2h_{AB} U^B du dx^A + h_{AB} dx^A dx^B; \quad (5.1)$$

where the metric variables U^A , and h_{AB} have the asymptotic expansions $U^A = L^A + \mathcal{O}(\mathcal{L})$, and $h_{AB} = H_{AB} + \mathcal{L}C_{AB} + \mathcal{O}(\mathcal{L}^2)$. We can always find coordinates $(u_B; \varphi_B; \psi_B; \mathbb{L}_B)$ (hereafter referred to as ‘inertial’ coordinates), and an associated conformal metric $dS_B^2 = \mathcal{L}^2 ds^2$ ($\mathcal{L} > 0$), such that (i) $\frac{\partial}{\partial u_B}$ is null and affine and points along the null generators of \mathcal{I}^+ , (ii) $\mathbb{L}_B = \mathcal{L} + \mathcal{O}(\mathcal{L}^2)$, (iii) the conformal metric in the subspace $(u_B = \text{const.}; \mathbb{L}_B = \text{const.})$ is the unit sphere metric on \mathcal{I}^+ . We fix a null-tetrad on \mathcal{I}^+ by choosing n^a to be affine and to point along the null generators of \mathcal{I}^+ and by choosing $m^{(a} m^{b)}$ to be the unit-sphere covariant metric in the 2-dimensional angular subspace. In inertial coordinates $(u_B; \varphi_B; \psi_B; \mathbb{L}_B)$ on \mathcal{I}^+ the tetrad has the form

$$n^a = (1; 0; 0; 0) \quad (5.2)$$

$$\bar{n}^a = (0; 0; 0; 1) \quad (5.3)$$

$$m^a = (0; \mathcal{P}^2; \mathcal{I}\mathcal{P}^2; 0); \quad (5.4)$$

where the tilde denotes a quantity defined with respect to inertial observers. Note that $\tilde{m}^{(A} \tilde{m}^{B)} = \mathcal{Q}^{AB}$ as required. We define a complex vector F^a , analogous to \tilde{m}^a (i.e. $F^{(A} F^{B)} = H^{AB}$), adapted to the coordinates used in the characteristic evolution code via

$$F^a = (0; F^A; 0); \quad (5.5)$$

where

$$F^A = \mathcal{Q}^A \frac{r}{\frac{K_0 + 1}{2}} - J_0 \mathcal{Q}^A \frac{s}{2(K_0 + 1)}; \quad (5.6)$$

where \mathcal{Q}^A is the dyad defined in Sec. III, $J_0 = \mathcal{Q}^A \mathcal{Q}^B H_{AB} = 2$, and $K_0 = \mathcal{Q}^A \mathcal{Q}^B H_{AB} = 2$. F^a and \tilde{m}^a are related by

$$\tilde{m}^a = e^{-\mathcal{I}} \mathcal{L} F^a + \tilde{n}^a; \quad (5.7)$$

The \tilde{n}^a term will not enter the News calculation.

To calculate the Bondi News one needs to evolve two scalar quantities \mathcal{L} , the phase factor in Eq. (5.7), and the conformal factor \mathcal{L} , as well the relations (φ_B) between the angular coordinates used in the characteristic evolution and inertial angular coordinates, and $u_B(u; \varphi_B)$ between the inertial time slicing and the time slicing of the characteristic evolution code. Then \mathcal{L} , (φ_B) , and $u_B(u; \varphi_B)$ are evolved using the following ODE’s along the null generators of \mathcal{I}^+

$$\frac{d}{du} \mathcal{L} = \frac{1}{2} \left(\frac{J_0 \mathcal{L} J_0}{K_0 + 1} + \frac{J_0 U_0 g J_0 + U_0 g J_0}{2(K_0 + 1)} + J_0 g U_0 + K_0 g U_0 + 2U_0 \right) \mathcal{L} \quad (5.8)$$

$$\frac{d}{du} \varphi_B = \frac{1}{2} (1 + \varphi_B) U_0 \quad (5.9)$$

$$\frac{du_B}{du} = \mathcal{L} e^{2H}; \quad (5.10)$$

where $U_0 = \mathcal{Q}_A L^A$. Also \mathcal{L} is evolved using the PDE

$$\partial_u \log \mathcal{L} = -U g \log \mathcal{L} + \frac{1}{2} g U \quad (5.11)$$

The Bondi News function up to a phase factor of $e^{-2\mathcal{I}}$ is given by

$$N = \frac{1}{2} \mathcal{L}^{-2} e^{2H} F^A F^B (\partial_u + L_L) C_{AB} - \frac{1}{2} C_{AB} D_C L^C + 2 \mathcal{L} D_A [\mathcal{L}^{-2} D_B (\mathcal{L} e^{2H})]; \quad (5.12)$$

where D_A is the covariant derivative with respect to H_{AB} . The Bondi News is calculated in three steps. First Eq. (5.12) is evaluated, ignoring the e^{2i} phase factor, as a function of the evolution coordinates $(u; \theta)$. Then using the relation (θ_B) , the News is interpolated onto a fixed inertial angular grid (i.e. $N(u; \theta_B)$) and multiplied by the phase factor e^{2i} (which is only known on the inertial grid). Finally, in post-processing, the News is interpolated in time onto fixed inertial time slices (i.e. $N(u_B; \theta_B)$). Once the News is obtained in inertial coordinates it can be decomposed into spin-weighted spherical harmonics.

VI. TESTS

We apply the algorithm described above to four simple tests. In the first set of tests (section VIA) the spacetime is Minkowski or a small perturbation of Minkowski. These tests are used to show the stability of the code and the errors due to transforming between the different coordinate systems and sets of variables. In the second set of tests (section VIB) the spacetime is that of a static spherically symmetric black hole. These tests indicate the accuracy of the code in non-trivial spacetimes.

In all cases the extracted gravitational wave signal should vanish identically. As this is true uniformly for all points at \mathcal{I}^+ we simplify the computation of the norms of the gravitational wave signals. When the results of the characteristic extraction are shown the norm used is the simple L_2 norm over all grid points at \mathcal{I}^+ , without any weighting by the area element. When we compute the wavesignal from the Zerilli approximation (see, e.g., [19, 20], and e.g. [21] for the implementation used here) we will use a norm over all angles,

$$(khk_2)^2 = \int_{\mathcal{I}^+} (h_+ - \bar{h}_+) (h_+ - \bar{h}_+)^Y d\Omega \quad (6.1)$$

$$= \frac{1}{(2r)^2} \int_{\mathcal{I}^+} (Q_m^+ - \bar{Q}_m^+) (Q_m^+ - \bar{Q}_m^+)^Y d\Omega \quad (6.2)$$

$$= \frac{1}{(2r)^2} \int_{\mathcal{I}^+} (Q_m^+ - \bar{Q}_m^+) (Q_m^+ - \bar{Q}_m^+)^Y d\Omega \quad (6.3)$$

where the last equality follows from the orthogonality of the spin-weighted tensor spherical harmonics. This gives a norm over all possible angles. In all our tests we expect $h_+ - \bar{h}_+$ to vanish for all angles so this norm should be identically zero. In what follows we shall look at the spherical harmonics up to $\ell = m = 7$ although in practice there is little contribution from the higher modes.

A. Flat spacetime

1. Minkowski

Minkowski space in standard coordinates is evolved in the harmonic Abigel code, retaining the analytic values on the Cauchy slice for all times. The domain runs from $x^1 \in [-10; 10]$, the extraction world tube is placed at $r = 7$, and the simulation is run until $t = 10$. The coarsest simulation used 50^3 points for the Cauchy grid and $35^2 = 31$ points for the characteristic grid. Simulations to test convergence scaled all grids by factors of 2.

This test indicates the level of numerical round off error in transforming from the Cauchy variables to the Bondi variables on the world-tube. As shown in Fig. 1, the extracted news is small in all cases but the level of truncation error increases linearly with the number of points on the extraction world-tube. Since the construction of the boundary data for the characteristic code involves derivatives of the Cauchy metric, this sensitivity to noise in the Cauchy data is expected. However, given the extremely low amplitude of the noise, it is unlikely that this will cause problems in practical simulations.

2. Random perturbations around Minkowski

This test is in the spirit of the robust stability tests of [3, 32, 33]. The stable evolution and extraction of white noise initial data with no frequency dependent growth of the wavesignal is a good indication that the combined evolution and extraction codes are stable. The domain runs from $x^1 \in [-10; 10]$, the extraction world tube is placed at $r = 7$, and the simulation is run until $t = 100$. The coarsest Cauchy grid has 51^3 points and the coarsest characteristic grid $35^2 = 31$ points.

The results in Fig. 2 show that the growth in the noise is independent of the resolution of both Cauchy and characteristic grids. This is strong evidence that the combined code is stable against small perturbations that in a practical run would be induced by numerical error.

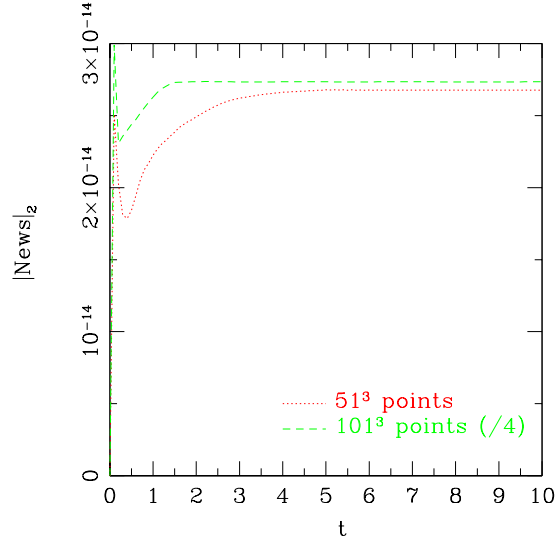


FIG. 1: The L_2 norm of the news for Minkowski space in standard coordinates. This indicates the level of numerical noise introduced by transforming variables on the world-tube. In this case the noise is linearly dependent on the number of points on the extraction world-tube. It is, however, extremely small.

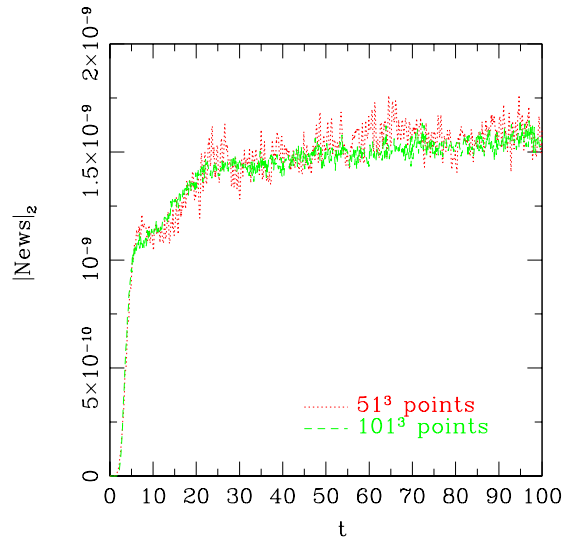


FIG. 2: The L_2 norm of the news for random perturbations of Minkowski where the Cauchy slice is evolved using the Abigel code. The news displays very slow growth that is independent of the frequency of the initial data. This is a good indication that the combined evolution and extraction method is stable.

B. BH spacetime

1. BH in a "centered" frame

To test a simple black hole spacetime we take the test used in [34] where a Schwarzschild black hole in ingoing Eddington-Finkelstein coordinates is used. The line element in the standard coordinates (\hat{t}, \hat{r}) is

$$ds^2 = -\left(1 - \frac{2M}{\hat{r}}\right) d\hat{t}^2 + \frac{4M}{\hat{r}} d\hat{t} d\hat{r} + \left(1 + \frac{2M}{\hat{r}}\right) d\hat{r}^2 + \hat{r}^2 d\Omega^2. \quad (6.4)$$

This is manifestly static in these coordinates. The spacetime is evolved using the BSSN code and excision methods described in [34]. The coarsest Cauchy grid has 29^3 points with $x^i = 0.4M$, whilst the characteristic grid has $35^2 \times 31$ points. The world-tube is at $r = 7M$. In the Cauchy evolution domain octant symmetry is used.

The evolution is only performed for a short time (to $t = 100M$) for simplicity. Over this timescale we see second order convergence for the news until $t = 7M$, as seen in Fig. 3. By varying the location of the world-tube we can see that the errors come from a variety of locations. At early times the error in the news is dominated by outgoing waves that converge at second order with the grid spacing. These are probably caused by finite differencing errors in the strong field regime. At late times the errors are dominated by incoming waves that do not converge. These are probably caused by the boundary conditions on the Cauchy grid which do not satisfy the constraints. As in [34] we are simply applying Sommerfeld type boundary conditions to all fields. This condition does not *a priori* satisfy the constraints and is not known to be well-posed. Thus we might expect errors to be induced by the use of these boundary conditions. It is likely that constraint satisfying boundary conditions or Cauchy-characteristic matching would solve or at least greatly reduce this problem.

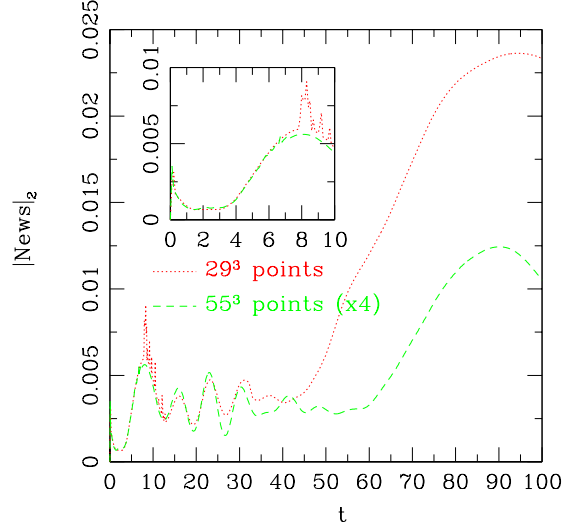


FIG. 3: The scaled L_2 norm of the news for a static spherically symmetric black hole where the Cauchy slice is evolved using the BSSN formalism. At early times, when the world-tube is causally disconnected from the outer boundary of the Cauchy slice the news converges to zero at second order as it should. Later, when the outer boundary is causally connected to the world-tube, deviations from second order convergence appear, indicating the effects of the Cauchy boundary conditions on the extracted wavesignal.

2. BH in an oscillating frame

The standard Schwarzschild black hole in ingoing Eddington-Finkelstein coordinates given in Eq. (6.4) is used. The moving coordinate frame $(t; x^i)$ is given by

$$t = \hat{t}; \quad x^i = \hat{x}^i + B^i b(t) \quad (6.5)$$

where B^i are parameters specifying the velocity and $b(t)$ is a simple periodic function turned on after some time $t > t_0$; here we use

$$b(t) = \begin{cases} 0; & t \leq t_0 \\ \sin((t - t_0)^3); & t > t_0 \end{cases} \quad (6.6)$$

For the test shown here we use $B^x = 0.2; B^y = 0.5; B^z = 0.3$ for the velocity and $\ell = 0.05; t_0 = 0.5$ for the function b .

The metric is given analytically on the Cauchy grid to avoid any boundary effects. The coarsest Cauchy grid has 51^3 points and covers the domain $x^i \in [-10M; 10M]$. The coarsest characteristic grid has $35^2 \times 31$ points. The extraction world-tube is at $r = 7M$. The simulation is evolved until $t = 100M$.

The news converges to zero as it should. However, Zerilli extraction does not give a signal that converges to zero as grid resolution is refined. Instead an erroneous non-trivial signal is computed. This error does converge to zero as $1=r^3$ as the location r of the detector, is increased.

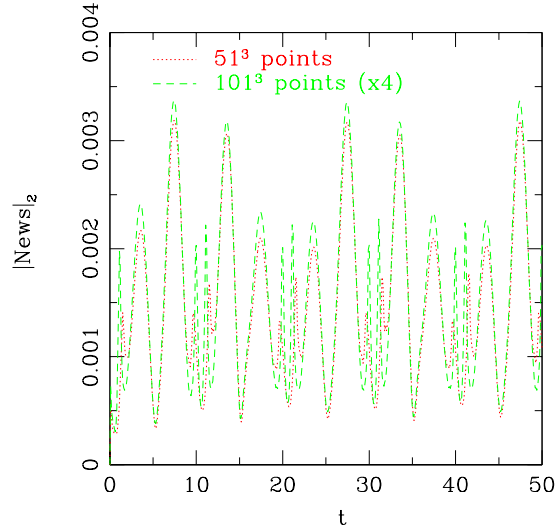


FIG. 4: The scaled L_2 norm of the news for a static spherically symmetric black hole in an oscillating frame. The news converges to zero at second order as it should.

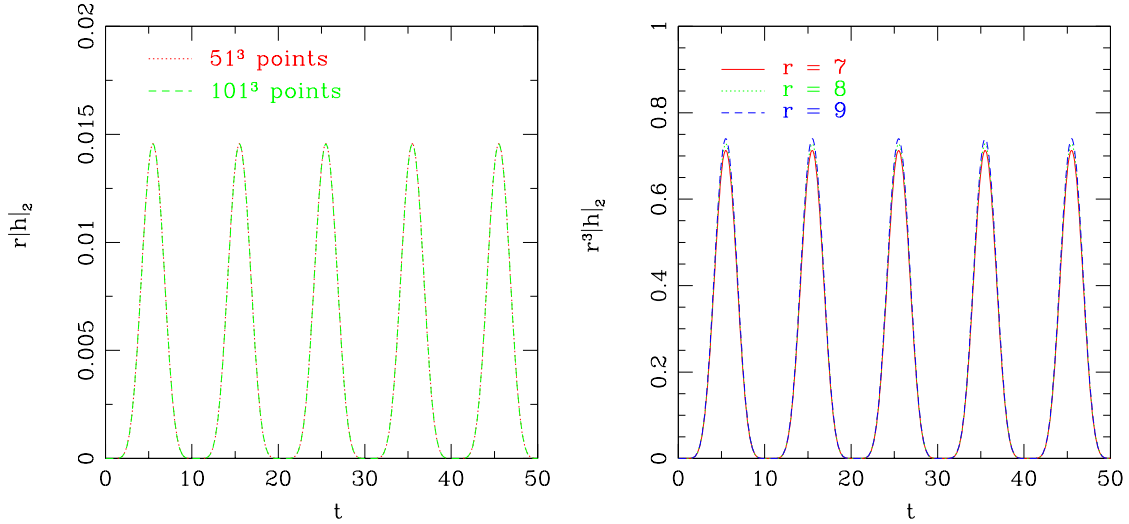


FIG. 5: The wavesignal computed using Zerilli extraction for the static spherically symmetric black hole in an oscillating frame. The “norm” is computed as described in the text with the radial dependence removed. The left panel shows that as the resolution of both the Cartesian grid and extraction sphere are increased the signal does not converge to zero. The right panel shows how this erroneous non-trivial wavesignal decays as r^2 as the radius of the detector is increased.

VII. CONCLUSIONS

We have demonstrated that it is possible to numerically extract the gravitational news at null infinity with existing codes in full 3D numerical relativity. The interface at the world-tube between the Cauchy and characteristic code works cleanly with both the BSSN and harmonic formulations as implemented by the codes detailed in [26] and [3, 27] respectively.

The extracted news is stable against small perturbations on the Cauchy grid, as shown in Sec. VI A 2 and the level of truncation error caused by transforming from the Cauchy slice to the characteristic slice will be negligible in practical calculations, as shown in Sec. VI A 1.

In non-trivial black hole spacetimes the code performs precisely as expected. In areas where perfect convergence of the news should be expected, such as the test in Sec. VI B 2 and the early time behavior of the test in Sec. VI B 1, such convergence is

found. However, when the BSSN outer boundary conditions on the Cauchy grid affect the data extracted on the world-tube this effect is clearly visible in the extracted news, as seen in the late time behavior in Sec. VIB 1.

Cauchy-characteristic extraction can be seen either as a first step towards a full Cauchy-characteristic matching code or as an improved gravitational wave extraction method in its own right. The results of this paper show that as a stand alone wave extraction method it produces the correct results in situations where other methods, such as Zerilli extraction, may fail. Such a situation is seen in Sec. VIB 2 where the Zerilli method fails to converge to the correct zero news due to the pure gauge motion of the center of mass.

However, as a practical method of extracting gravitational waves there remain limitations on Cauchy-characteristic extraction. One is clearly seen in the test of Sec. VIB 1; the method is extremely sensitive to errors on the Cauchy slice, particularly those induced by inconsistent Cauchy boundary conditions. Another limitation that is inherent in all characteristic formulations is that the code will break down if the coordinate system forms caustics. This does not happen when the worldtube is sufficiently far out, e.g. in the regime where perturbative extraction would be valid. An explicit example of this problem is that the algorithm will break if $r_c < 0$; that is, if the world-tube is not timelike then caustics form on the world-tube itself. In the tests performed here only the first restriction due to the Cauchy boundary conditions has caused problems. However, in situations where the gauge on the Cauchy slice is very dynamical, the world-tube at a fixed coordinate radius may not remain timelike.

Acknowledgments

We are grateful to Nigel Bishop for help at the start of this project. Also, we are thankful to Jeff Winicour for his support throughout the project as well for his careful reading of the manuscript. Computer simulations were done at the PEYOTE cluster of the Albert Einstein Institut in Golm, Germany and at the Pittsburgh Supercomputing Center which was supporting this project under grant PHY040015P. While importing the extraction code into the Cactus infrastructure we have benefited from the support of the Cactus team for which we are grateful.

We thank the Luisiana State University for their hospitality. MB was supported by the National Science Foundation under grant PHY-0244673 to the University of Pittsburgh. BSz was partially supported by the National Science Foundation under grant PHY-0244673 to the University of Pittsburgh. IH was partially supported by PPARC grant PPA/G/S/2002/00531.

-
- [1] R. Gómez, R. Marsa, and J. Winicour, Phys. Rev. D **56**, 6310 (1997), gr-qc/9708002.
 - [2] N. Bishop, R. Gomez, P. Holvorcem, R. Matzner, P. Papadopoulos, and J. Winicour, J. Comp. Phys. **136**, 140 (1997).
 - [3] B. Szilagyi, B. Schmidt, and J. Winicour, Phys. Rev. D **65**, 064015 (2002), gr-qc/0106026.
 - [4] L. Lehner, J. Comp. Phys. **149**, 59 (1999).
 - [5] L. Lehner, Ph.D. thesis, University of Pittsburgh (1998).
 - [6] N. T. Bishop, R. Gómez, L. Lehner, and J. Winicour, Phys. Rev. D **54**, 6153 (1996).
 - [7] R. Gómez, L. Lehner, R. Marsa, and J. Winicour, Phys. Rev. D **57**, 4778 (1998), gr-qc/9710138.
 - [8] N. T. Bishop, R. Gómez, L. Lehner, M. Maharaj, and J. Winicour, Phys. Rev. D **56**, 6298 (1997), gr-qc/9708065.
 - [9] R. Gómez, Phys. Rev. D **64**, 024007 (2001).
 - [10] J. Winicour, Living Reviews in Relativity **1**, 5 (1998), [Online article].
 - [11] N. Bishop, R. Isaacson, R. Gómez, L. Lenher, B. Szilágyi, and J. Winicour, in *Black Holes, Gravitational Radiation and the Universe*, edited by B. Iyer and B. Bhawal (Kluwer, Dordrecht, The Netherlands, 1999), p. 393.
 - [12] B. Szilágyi, Ph.D. thesis, University of Pittsburgh (2000).
 - [13] Y. Zlochower, Ph.D. thesis, University of Pittsburgh (2002).
 - [14] Y. Zlochower, R. Gomez, S. Husa, L. Lenher, and J. Winicour, Phys. Rev. D **68**, 084014 (2003).
 - [15] G. Allen, W. Bengert, T. Goodale, H. Hege, G. Lanfermann, A. Merzky, T. Radke, E. Seidel, and J. Shalf, Cluster Computing **4**, 179 (2001), <http://www.cactuscode.org/Papers/CactusTools.ps.gz>, <http://www.cactuscode.org/Papers/CactusTools.ps.gz>.
 - [16] G. Allen, W. Bengert, T. Dramlitsch, T. Goodale, H. Hege, G. Lanfermann, A. Merzky, T. Radke, and E. Seidel, in *Europar 2001: Parallel Processing, Proceedings of 7th International Conference Manchester, UK August 28-31, 2001*, edited by R. Sakellariou, J. Keane, J. Gurd, and L. Freeman (Springer, 2001), <http://www.cactuscode.org/Papers/Europar01.ps.gz>.
 - [17] Cactus, <http://www.cactuscode.org>.
 - [18] T. Goodale, G. Allen, G. Lanfermann, J. Massó, T. Radke, E. Seidel, and J. Shalf, in *Vector and Parallel Processing - VECPAR'2002, 5th International Conference, Lecture Notes in Computer Science* (Springer, Berlin, 2003).
 - [19] F. J. Zerilli, Phys. Rev. Lett. **24**, 737 (1970).
 - [20] V. Moncrief, Annals of Physics **88**, 323 (1974).
 - [21] K. Camarda and E. Seidel, Phys. Rev. D **59**, 064019 (1999), gr-qc/9805099.
 - [22] N. T. Bishop, R. Isaacson, R. Gómez, L. Lehner, B. Szilagyi, and J. Winicour, in *On the Black Hole Trail*, edited by B. Iyer and B. Bhawal (Kluwer, 1998), gr-qc/9801070.
 - [23] R. Arnowitt, S. Deser, and C. W. Misner, in *Gravitation: An Introduction to Current Research*, edited by L. Witten (John Wiley, New York, 1962), pp. 227–265, gr-qc/0405109.

- [24] M. Shibata and T. Nakamura, Phys. Rev. D **52**, 5428 (1995).
- [25] T. W. Baumgarte and S. L. Shapiro, Phys. Rev. D **59**, 024007 (1999), gr-qc/9810065.
- [26] M. Alcubierre, B. Brügmann, P. Diener, M. Koppitz, D. Pollney, E. Seidel, and R. Takahashi, Phys. Rev. D **67**, 084023 (2003), gr-qc/0206072.
- [27] B. Szilágyi and J. Winicour, Phys. Rev. D **68**, 041501 (2002), gr-qc/0205044.
- [28] H. Bondi, F. Sachs., M. G. J. van der Burg, and A. W. K. Metzner, Proc. R. Soc. **A269**, 21 (1962).
- [29] R. Sachs, Proc. Roy. Soc. London **A270**, 103 (1962).
- [30] R. Gómez, L. Lehner, P. Papadopoulos, and J. Winicour, Class. Quantum Grav. **14**, 977 (1997), gr-qc/9702002.
- [31] N. Bishop and S. Deshingkar, Phys. Rev. D **68**, 024031 (2003).
- [32] B. Szilágyi, R. Gómez, N. T. Bishop, and J. Winicour, Phys. Rev. D **62**, 104006 (2000), gr-qc/9912030.
- [33] M. Alcubierre, G. Allen, T. W. Baumgarte, C. Bona, D. Fiske, T. Goodale, F. S. Guzmán, I. Hawke, S. Hawley, S. Husa, et al., Class. Quantum Grav. **21**, 589 (2004), gr-qc/0305023.
- [34] M. Alcubierre and B. Brügmann, Phys. Rev. D **63**, 104006 (2001), gr-qc/0008067.
- [35] P. Hübner, Class. Quantum Grav. **18**, 1871 (2001).
- [36] J. Frauendiener, Living Rev. Relativity **7** (2004), <http://www.livingreviews.org/lrr-2004-1>.
- [37] S. Husa, in *Proceedings of the 2001 Spanish Relativity meeting*, edited by L. Fernández and L. M. González (Springer, 2003), vol. 617 of *Lecture Notes in Physics*, pp. 159–192.
- [38] It is not always necessary to evolve spacetime to $t = 1$ in order to obtain the information at \mathcal{I}^+ . For example, if a *hyperboloidal* slicing is used (see, e.g., [35] and [36, 37] for reviews) then information propagates to \mathcal{I}^+ in finite time.